RSC Advances

ROYAL SOCIETY OF CHEMISTRY

www.rsc.org/advances

Protein-Concentration-Dependent Adsorption Behaviour of Inorganic Layered Materials

Victor Wei-Keh Chao(Wu),[§, 5, 6] Chao-Chen Hsu,[1, 2, 3, 7] Wei-Ming Lu,[1, 2] Wen-Jing Chen,[1, 2] Bunekar Naveen,[1, 2] Tsung-Yen Tsai,*[, 1, 2, 3, 4]

[1]Department of Chemistry, [2]Center for Nanotechnology, [3]Institute of Biomedical Technology, [4]Master Program in Nanotechnology, of Chung Yuan Christian University, Chung-Li, Taiwan 32023, Republic of China,

[5]Department of Chemical and Materials Engineering, National Kaohsiung University of Applied Sciences, Jian-Gong Road, San-Ming Section, Kaohsiung 80782, Taiwan, Republic of China,

[6] Victor Basic Research Laboratory e. V. Gadderbaumer-Strasse 22, D-33602 Bielefeld, Germany.

[7]Institute of Nuclear Energy Research, Atomic Energy Council, 1000, Wenhua Road, Lungtan, Taoyuan 325, Taiwan

*To whom correspondence should be addressed.

Tel: +886-3-2653342

Fax: +886-3-2653399

Email: yen@cycu.edu.tw

§Co-corresponding author

Abstract

The adsorption of six smectite clay minerals with different structures (either octahedrally or tetrahedrally substituted) and MgAl layered-double hydroxides (MgAl-LDHs) was measured at two different pH values (e.g., 2.5 and 9.5) and at different concentrations of the Bovine Serum Albumin (BSA) protein. Clays used in this study are layered materials of different ion-exchange capacities (IEC). BSA solutions were prepared at different concentrations; these were then adsorbed on the gallery of the layered materials up to saturation. The relative concentrations were systematically changed and screened to obtain the optimal adsorbance. The effects of the BSA concentration and pH on adsorption, interaction on the surface, edge, and interlayer of the materials were monitored with X-Ray diffraction (XRD), transmission electron microscopy (TEM), Fourier transformed Infrared spectrometry (FT-IR), and thermogravimetric analysis (TGA); the results of these analyses were discussed in details. The clay materials revealed high adsorption capacities under static conditions; BSA was mainly adsorbed via electrostatic interactions. A correlation between the distance between the layers and the adsorbed quantity of BSA was found. Finally, our results showed that, for an optimal intercalation of BSA into the smectite clay minerals and MgAl-LDH, the layer distances must increase up to approximately 65 and 5.07 Å, respectively.

1. Introduction

Naturally abundant clay minerals and their new hybrid materials have recently attracted increasing academic interest owing to their unique physicochemical properties and potential applications.[1-7] The development of inorganic and biomaterial hybrids, including proteins and nucleic acids, generates new materials with biological functions. Clay minerals[1-3,7-9] play a critical role in the binding and adsorption of proteins because of their peculiar properties such as surface area, ionic-exchange capacity (IEC, Table 1), charge density, degree of swelling,[3] intercalation,[1-3,5] and adsorption.

Natural clay minerals, particularly smectite clay, are environmentally friendly, inexpensive, and abundant; in addition, they typically show high binding capacities for proteins and have properties similar to those of natural cation exchangers. They can be classified as 2:1 layered clays and have a repetitive structure of one octahedral layer fixed between two tetrahedral layers; di- or trivalent and tri- or tetravalent ions are present in the octahedral and tetrahedral layers, respectively.[7-9] These ions are all substituable. For instance, in the case of montmorillonite, Al^{3+} ions in the octahedral layers can be partially substituted with Mg^{2+}. Such substitutions result in net negative charges, which are compensable by the cations in the interlayer space.[10-18] Owing to their particular layer structure (e.g. montmorillonite), which exhibits negative surface charges, they can be used as ion exchangers or in chromatography to purify or isolate specific proteins and

biomolecules. Thus, smectite clay represents a valid alternative to cation-exchange resins, especially for the isolation or purification of proteins and enzymes for technical applications.[6,7,19] Owing to these properties, it is suitable for the adsorption of not only proteins but also biologically active molecules such as alkaloids,[19,20] nucleic acids,[21,22] nitroaromatic compounds,[23,24] viruses,[25-27] and chlorinated phenols.[1]

The adsorption of proteins has been studied using α-zirconium phosphate;[28-30] adsorption of proteins and cells[31-34] has been investigated with montmorillonite and related layered clays.[9] Layered double hydroxides (LDHs) or sheets,[5,7] which can be chemically synthesized and are similar to clay minerals, are a class of ionic-lamellar compounds that consist of positively charged brucite-like layers with an interlayer region containing charge-compensating anions and solvent molecules. Several studies[35-37] were carried out to not only meet an increasing demand from the market, but also improve the environmentally friendly production process[1,2,4,38,39] and simplify the recycling of the materials. The costs of isolation and purification of proteins form a substantive part (40%–80%) of the overall cost of protein production. Therefore, protein immobilisation on solid surfaces of smectic clay is of particular interest.[28] The layers of these inorganic solids can be easily expanded to accommodate the protein in their galleries. Moreover, a number of proteins of different sizes can be selectively intercalated[1-3,5] into these galleries, in which proteins retain their structures to a significant extent.[28,29] Therefore, the weight and size of proteins are critical parameters for

adsorption on these clay materials. For instance, Zhou et al.[9] have demonstrated that smaller insecticidal protein molecules can be intercalated into the gallery region of montmorillonite, whereas larger insecticidal protein molecules are adsorbed on the surface of the solid; in this case, the layered material functions as a uniform support, thereby enhancing the stability of the protein. Kumar et al.[30] reported that proteins are sensitive to the pH and temperature of their environment; for example, they are unstable in organic solvents. These problems can be overcome if the protein molecules are adsorbed in inorganic-layered materials, which may also be employed as biocatalysts and biosensors.[1-3,5,40,41] Intercalation characteristics of clays, modified clays, or smectites can also be used for protecting the environment from pollutants.[1-3]

Bovine serum albumin (BSA) is a relatively inexpensive protein that has been widely investigated and extensively used as one of the "standard" protein molecules for research purposes. Therefore, BSA was chosen for the present study; we focused on its adsorption behaviour on six different clay-based inorganic layered materials along with MgAl-LDH. The adsorption amount, dispersion morphology, and swellability of BSA on the inorganic-layered materials were studied. Finally, based on our results, we suggest a more efficient method for the purification of BSA.[42]

2. Experimental

2.1. Clay Materials

The following list includes the six different montmorillonite layered clays that were used in this study:

1. CL5 (Sumecton-SA) [$Na_{0.49}Mg_{0.14}(Mg_{5.97}Al_{0.03})(Si_{7.20}Al_{0.80})O_{20}(OH)_4 \cdot nH_2O$] (purchased from Kunimine Ltd.),
2. CL42 (PK-802) [$Na_{0.89}(Al_{3.11}Mg_{0.89})\ Si_8O_{20}(OH)_4 \cdot 1.75H_2O$] (from PAI KONG Nanotechnology Co.),
3. CL120 (NTC-C34) [$Ca_{0.31}Na_{0.07}\ (Al_{3.31}Mg_{0.69})Si_8O_{20}(OH)_4 \cdot 2.148H_2O$] (from China Glaze Co.),
4. CL88 (NTC-C02) [$Ca_{0.54}Na_{0.12}(Al_{2.8}Mg_{0.77}\ Fe_{0.43})Si_8O_{20}(OH)_4 \cdot 0.34H_2O$] (from China Glaze Co.),
5. CL111 (Cloisite Na^+) [$(Na, Ca)_{0.66}(Al, Mg)_4Si_8O_{20}(OH)_4 \cdot nH_2O$] (from Southern Clay Products Co.),
6. CL22 (PGW) [$Na_{1.10}(Al_{2.90}Fe_{0.30}Mg_{0.8})Si_8O_{20}(OH)_4 \cdot H_2O$] (from Nanocor Co. Ltd.).

The properties of these systems were analysed; results are shown in Fig. 1 and Table 2.

2.2. Synthesis of MgAl-LDH

Highly dispersed MgAl-LDH was prepared hydrothermally according to a typical procedure (Scheme 1). In particular, 3.85 g (0.015 mol) of $Mg(NO_3)_2 \cdot 6H_2O$ (purchased from Sigma-Aldrich) and 2.82 g (7.5×10^{-3} mol) $Al(NO_3)_3 \cdot 9H_2O$ (from J. T. Baker) were dissolved in 30 mL of deionised water, and 2.4 g (0.06 mol) NaOH (from SHOWA) were dissolved in 30 mL of deionised water. Then both were mixed together. The resulting mixture (adjusted to pH = 10) was stirred for nucleation for 2 min and aged at 80 °C for 13 h. The final precipitate was collected by centrifugation at 7000 rpm and washed with deionised water, followed by desiccation under vacuum for 24 h.

2.3. Adsorption and Intercalation of BSA

Firstly, 0.02 M of phosphate buffer solutions in deionised water at pH = 2.5 and 9.5 were prepared. Intercalation and adsorption experiments were performed on the buffer solutions containing BSA molecules adsorbed into the six inorganic layered clay materials or MgAl-LDH at a pH of 2.5 and 9.5, respectively. Six BSA solutions of different concentrations were prepared, i.e., 15, 30, 45, 60, 75, and 90 mg of BSA in 0.75 mL of the buffer solution (the concentration of the sample prepared with 15 mg corresponds to 2.885×10^{-4} M). In addition, 15 mg of each of the six purchased clay and prepared MgAl-LDH materials was dissolved into 0.75 mL of the phosphate

buffer solution at pH = 2.5 and 9.5, respectively. Each of the solutions containing 15 mg of clay or MgAl-LDH was then mixed with the six different BSA solutions. This resulted in one adsorption set of 6 × 6 = 36 samples at pH = 2.5 and one set of 6 × 1 = 6 samples at pH = 9.5 prepared for the MgAl-LDH (Scheme 2). All the mixtures were mixed at 4 ºC for 24 h. The relative concentrations of the suspensions with BSA/clay were 1, 2, 3, 4, 5, 6 (in mass ratio, mg/mg). They were centrifuged at 14000 rpm for 5 min, then washed several times with fresh buffers to remove the floating proteins, and finally freeze-dried.

2.4. Characterisation of the Materials

The thermal stability and adsorption behaviour of BSA adsorbed onto the clays were measured by thermogravimetric analysis (TGA). These measurements were performed with a TG/DTA 6200 system under gas flow at a temperature range of 40 and 900 ºC with a scan rate of 10 ºC/min. Wide angle X-ray diffraction (WAXD) was carried out with a PANalytical (X'Pert Pro PW3040/60) under 45 KV, 40 mA, wavelength λ = 1.54 Å (Cu-Kα), with a scan range of $2° < 2\theta < 80°$ and speed of 3º/min. Transmission electron microscopic (TEM) images with magnification of 50 K and 100 K were obtained with a JEOL (JEM-2010FX) microscope at an acceleration voltage of 200 KV. Using an ultra-microtome with a diamond knife, we prepared the samples (thickness of about 100 nm) for the TEM measurements at room temperature. Fourier transformed Infrared spectrometry

(FT-IR) of the samples in KBr pellets was performed on a JASCO, FTIR-4200 Type A spectrometer.

3. Results and Discussion

3.1. Properties of the inorganically layered materials

The swellability of the inorganically layered materials studied in this work is shown in Fig. 1 and Table 1. In particular, 2 g of each of the seven compounds (six different clays and MgAl-LDH) was added into a graduated cylinder with 100 mL distilled water for 8 h. The sediment volume (in mL/2g) can be obtained from the graduation of the cylinder. This unit was chosen for the welling ability tests on the seven studied compounds.[1] Among all six clay solutions, that of CL5 was the clearest, indicating that the laminated structure of CL5 was completely dispersed in the aqueous solution. In addition, distinguishable borderlines between sedimentation and suspension parts were observed for the remaining solutions, indicating the swellability of CL42, CL120, CL88, CL111, and CL22. The borderline becomes very clear in the case of MgAl-LDH, i.e., the laminated structure of MgAl-LDH in aqueous solution showed the lowest swellability, due to the strongest ionic attractions between the laminated layers.

3.2. Adsorption behaviour of BSA on the inorganic layered materials

The capability of the studied laminated inorganic materials to adsorb BSA molecules (Scheme 3) was investigated. The adsorption capacity and residual amount of the inorganic laminated material were evaluated using TGA (Figs. 2 and 8). Our results showed that the amount of adsorbed BSA in mg relative to g of clay is proportional to the concentration of BSA in the buffer solution (Fig. 2). The adsorbed quantity of BSA increases by about 2.5 times as the BSA concentration is increased from 1 to 6 (where the indexes 1–6 correspond to 15–90 mg of BSA mixed with 15 mg of clay). The saturation adsorption occurs at a BSA concentration of 5 (75 mg). The adsorbed amounts of BSA at a BSA concentration of 6 were 83 mg/g and 63 mg/g for CL42 and CL22, respectively; this is higher than those measured at a BSA concentration of 5. In contrast, the adsorbed amounts of BSA were 116 mg/g and 38 mg/g for CL111 and CL88, respectively, which are smaller than those at the BSA concentration of 5. This adsorption behaviour may be influenced by the ionic strength of the clay, charge density, and protein-protein lateral repulsion. The saturation adsorption of BSA on the laminated interlayer surfaces of clay may be induced by Langmuir-type adsorptions.[43-45] There can be either a monolayer or multilayer adsorption of BSA, depending on the interlayer spacing.[43-45] Gesture, crowdedness, and distribution of the adsorbed BSA molecules on the surface can be estimated.[43-45]

Regarding MgAl-LDH, the adsorption of the BSA molecules was tested in a buffer solution at pH = 9.5, which maximises the adsorption of the negatively charged BSA molecules. The adsorption was found to be significantly lower than those of all studied clays, except for CL5 (Table 1). MgAl-LDH of layered material has poor swelling properties, even in water-soluble liquids. Because the interlayer gaps in MgAl-LDH are too small, BSA is almost exclusively adsorbed onto its external surfaces.

The adsorption curves obtained in this work are characterised by small uncertainties, i.e., the adsorption experiments can be well reproduced, and the bidirectional dynamic-balance phenomena can be observed. CL111, CL120, and CL88 systems showed similar adsorption capacities and efficiencies. CL42, CL22, CL111, CL120, and CL88 showed a higher adsorption stability and capacity than those of CL5. All these materials showed approximately adsorption capacities that are about 20 times higher than that of MgAl-DLH at a BSA concentration range of 1 and 6. Additionally, charge distributions within the interspacing, size, orientation, and conformation of the adsorbed protein molecules[43-45] may also be important factors that affect the different adsorption behaviour observed for the studied clays.

The charge distributions of CL111, CL42, CL22, CL120, and CL88 octahedral clays (Table 1) selected for our experiments showed different IEC values. The cationic-exchange capacity was virtually unchanged at relative BSA concentrations of 1.0 or 2.0 folds as well as 1/1 – 2/1 folds. The cationic exchange takes place only within the interlayers of the clays; at this stage, the BSA molecules are not completely adsorbed into the interlayers. Thus, as the relative concentration of BSA is gradually increased, the substitutable vacancies available in interlayers can be occupied. The adsorption steadily increases up to a concentration of 5 (15 × 5 mg of BSA in the mixture with 15 mg of clay), and reaches saturation at a concentration of 6. The charge distributions and IEC of the six clays and MgAl-DLH are listed in Table 1. In the case of MgAl-LDH, the electrostatic attraction between the nanosheets and BSA molecules are 3–5 stronger than those with the other six clays (Table 2); these are expected to result in an adsorption well. However, MgAl-LDH swellability is approximately only half of all six clays; this results in an adsorption capability and ability of only 1/10 compared to those of the other six clays.

A gradual replacement with BSA and an increase in the BSA content lead to an increase in the distance between the layers, thereby reducing the unit area of the layer surface occupied by one BSA molecule.[43-45] The orientation of BSA can also be altered, from laying to standing.[43-45] An adjustment of the surface negative charge density of the six clays may even increase the amount of

adsorbed BSA molecules as well as the density of the BSA molecules per unit area on the layer surface.

CL42, CL22, CL120, and CL88 showed saturation adsorptions at a BSA concentration of 6, with the adsorption being proportional to IEC (Table 1). In contrast, CL111 shows a rather weaker adsorption at this BSA concentration. In particular, its adsorption curve decreases and is lower than the saturation asymptote. The attraction of CL111 is weaker than those of the clays with a higher IEC in the interlayers. Because ionic charges are less available (IEC = 92, Table 1) for substitution, the adsorption cannot reach the optimal level of saturation adsorption. CL42 shows the highest adsorption capability (2224 mg/g, Table 1) and the highest electrostatic attraction between the layers among all clays, along with the strongest cationic-exchange capacity. Therefore, CL42 was chosen to study the adsorption behaviour of BSA at different pH values (Fig. 3). It was found that adsorption is larger at lower pH values (e.g., 2.5); at the isoelectric point, e.g., pI = pH 4.70 of BSA (Fig. 3), the adsorption amount is approximately 1400 mg/g. The adsorption amount at pH = 9.5, approximately 1200 mg/g, is smaller than that at pH value of = 4.70. However, it is not close to zero, as it should be ideally. The following reasons may explain this behaviour: 1. The interactions between BSA and the surfaces, including the edges of the interlayers, cannot completely be induced by pure electrostatics; hydrogen-bonding and van der Waals interactions should also contribute. 2.

The concentrations of BSA/clay = 0/1 – 5/1 (Table 1) are too high, and the effect of the pH on adsorption[42-45] and desorption[42, 46] of BSA by the smectite clay minerals cannot be observed. The relative concentration of BSA should be thus reduced to values lower than 1/5.

3.3. Adsorption patterns of BSA on the inorganic layered materials

The theoretical particle size of BSA is about 40 × 40 × 140 $Å^3$, with the structure being dependent on the pH and temperature. The interlayer distance of the pure natural clay is about 12–13 Å (Tables 1 and 2). The WAXD results suggest that CL42 reaches the optimal crystalline form (compared to other clays CL120, CL111, CL22, and CL88) for 1/1 BSA/clay samples (Fig. 4). CL42 shows the highest swellability (100 mL/2g of clay) and the best saturation adsorption (2224 mg/g, Table 1).

Fig. 5 shows an increase in the layer spacing of the octahedrally substituted clays as a function of the BSA concentration. As the BSA molecules are inserted into the interlayers, the interlayer distances steadily increase, weakening the ionic attraction between layers. Because the insertion of the BSA molecules is irregular, the quasi-parallel layers of the clay are slanted. A comparison of the size of BSA (approximately 40 Å) with the distances between the layers in the clay (Table 1) suggests that a monolayer adsorption is possible in the concentration range 1/1–6/1. Thus, the

higher the BSA concentration, the more crowded the BSA molecules into the layer, this resulting in a nearly standing orientation.[43-45]

As shown in Fig. 6, no peaks were found in the WAXD patterns of the BSA/CL5 mixture, with the BSA concentration ranging from 0/1 (pure CL5) to 5/1. The adsorption of BSA may thus occur irregularly. In addition, the TEM analysis revealed dark grey strips, indicating peeling-off structures of CL5 mixed with BSA (Figs. 7a and 7b). The TGA curves (Fig. 8) of CL5 (pure and mixed with BSA, concentration of 5/1), show that the pure CL5 is stable at temperatures as high as 900 ºC, i.e., significantly more stable than the mixture. The weight reduction of 5.96% observed at 200 ºC may be caused by the vaporisation of water on the surface; the reduction of 67.86% at 900 ºC may be due to the adsorption of the BSA molecules. This suggests that the BSA molecules are adsorbed on the surfaces of the interlayers of the CL5 material.

Fig. 9 shows the FT-IR spectra of pure CL5 along with those of the CL5/BSA mixture (concentration of 5/1). The typical bands of CL5 were clearly observed. In particular, the broad peaks of the relative transmissions around 463 cm^{-1}, 518 cm^{-1}, and 1036 cm^{-1} were assigned to the stretching bands of Mg-O, Al-O, and Si-O, respectively. Transmissions of water bending and O-H stretching vibrations were found at 1641 cm^{-1} and 3436 cm^{-1}, respectively. Upon adsorption of BSA

into the CL5 interlayers, a strong adsorption band around 2948 cm^{-1} appeared that was assigned to the C-H stretching vibrations; bands at 1394 cm^{-1} and 1452 cm^{-1}, and at 1524 cm^{-1} and 1660 cm^{-1} were assigned to the COO^- stretching modes and to carbonyl groups, respectively. These data confirmed that the BSA molecules were successfully adsorbed at pH = 2.5.

The WAXD patterns in Fig. 10 show that, upon adsorption of BSA at a concentration range of 1/1 and 5/1, the interlayer distances of MgAl-LDH proportionally increase, from 26.58 to 31.65 Å (Table 1). These data suggest that the BSA molecules do not enter the interlayers, but they are adsorbed on the surfaces and edges of the interlayers, leading to a thickness increase up to 5.07 Å.

The stepwise adsorption and intercalation of BSA on layered materials is illustrated in Scheme 1. The BSA adsorption into the interlayers of the inorganic layered materials (CL42, 120, 111, CL22, and CL88) (Figs. 4 and 5) and on the surface of MgAl-DLH (Fig. 10) was clearly observed in our XRD experiments. In addition, phenomena of exfoliation after adsorption of BSA by CL5 were demonstrated with TEM (Fig. 7) and XRD (Fig. 8).

4. Conclusion

The properties and functional behaviour (e.g., IEC, swellability, saturation adsorption, and intercalation) of smectite clay minerals, namely CL111, CL42, CL22, CL120, CL88, and CL5 (the latter is tetrahedrally substituted; all the other clays are octahedrally substituted, Table 1), were studied and compared to those of synthetic MgAl-LDH for protein adsorption. MgAl-LDH shows an adsorption as low as 258 mg of BSA (with 1 g LDH). CL5 shows peeling-off behaviour and is not sufficiently stable for adsorption (Figs. 6–8). CL111, CL42, CL22, CL120, and CL88 (Figs. 2–5) showed suitable properties for intercalation and adsorption; these are desirable features for a selective analysis and purification. Among all studied clays, CL42 (Figs. 3 and 4) shows the highest saturation adsorption (2224 mg/g) and can thus be optimised[46] to be used as a cationic exchanger. In addition, it was found that protein adsorption can be induced by electrostatic interactions and its weight can be significantly increased by a suitable optimisation and/or modification of the interlayer surface of the clay.[46]

Hydrophobic interactions, hydrogen bonding, and van der Waals forces may be involved in protein adsorption on the surfaces of layers of all clays and sheets of MgAl-LDH. Protein adsorption and selective adsorption on MgAl-LDH are rather weak, because the interlayers are not sufficiently flexible and cannot adapt to the size of the protein.

WAXD patterns (Figs. 4 and 5) indicate that the protein adsorption via intercalation is more probable, because the octahedrally substituted smectite clay minerals may induce multilayer adsorptions. Thus, our data suggest that these materials may be suitable not only for protein adsorption, but also for separation and purification. Finally, based on the results presented in this work, we expect that the laminated layers of these materials may be suitable for a diverse range of methods related to adsorption and desorption[46] such as exchange, purification, and analysis.[42]

Acknowledgement

The authors would like to thank China Glaze group for providing the clays.

References

1. R. C. Zielke and T. J. Pinnavaia, *Clays and Clay Minerals*, 1988, 36, 403-408.
2. M. Kowalska, H. Güler, and D. L. Cocke, *Sci. Total Environment*, 1994, 141, 223–240.
3. J. Bujdák, M. Janek, J. Madejová, and P. Komadel, *J. Chem. Soc. Faraday Trans.*1998, 94, 3487-3492.
4. J. H. Pan, X. Zhang, A. J. Du, H. Bai, J. Ng, and D. Sun, *Phys. Chem. Chem. Phys.* 2012, 14, 7481-7489.
5. Y. Liu, N. Wang, J. H. Pan, F. Steinbach, and J. Caro, *J. Am. Chem. Soc.* 2014, 136, 14353-14356.
6. K. Ralla, U. Sohling, D. Riechers, C. Kasper, F. Ruf and T. Scheper, *Bioprocess. Biosyst. Eng.*, 2010, 33, 847-861.
7. Q. Wang and D. O'Hare, *Chem. Rev.*, 2012, 112, 4124-4155.
8. S. Servagent-Noinville, M. Revault, H. Quiquampoix and M. H. Baron, *J. Colloid Interface Sci.*, 2000, 221, 273-283.
9. X. Zhou, Q. Huang, S. Chen and Z. Yu, *Appl. Clay Sci.*, 2005, 30, 87-93.
10. M. K. Arimitsu Usuki, Yoshitsugu Kojima, Akane Okada, Toshio Kurauchi and Osami Kamigaito, *J. Mater. Res.*, 1993, 8, 1174-1178.
11. J. L. Bonczek, W. G. Harris and P. Nkedi-Kizza, *Clay Clay Min.*, 2002, 50, 11-17.
12. F. Cavani, F. Trifirò and A. Vaccari, *Catal. Today*, 1991, 11, 173-301.
13. F. Leroux and J.-P. Besse, *Chem. Mat.*, 2001, 13, 3507-3515.
14. P. Maiti, *Langmuir*, 2003, 19, 5502-5510.
15. S. Miyata, *Clay Clay Min.*, 1983, 31, 305-311.

16. S. Miyata, *Clay Clay Min.*, 1980, 28, 50-56.

17. L. A. Utracki, M. Sepehr and E. Boccaleri, *Polym. Adv. Technol.*, 2007, 18, 1-37.

18. V. Botella, V. Timon, E. Escamilla-Roa, A. Hernández-Languna and C. I. Sainz-Díaz, *Phys. Chem. Miner.*, 2004, 31, 475-486.

19. H. J. Huebner, S. L. Lemke, S. E. Ottinger, K. Mayura and T. D. Phillips, *Food Addit. Contam.*, 1999, 16, 159-171.

20. E. COHEN, T. JOSEPH, I. LAPIDES and S. YARIV, *Clay Min.*, 2005, 40, 223-232.

21. G. Pietramellara, M. Franchi, E. Gallori and P. Nannipieri, *Biol. Fertil. Soils*, 2001, 33, 402-409.

22. G. Pietramellara, J. Ascher, M. Ceccherini, P. Nannipieri and D. Wenderoth, *Biol. Fertil. Soils*, 2007, 43, 731-739.

23. K. W. Weissmahr, S. B. Haderlein, R. P. Schwarzenbach, R. Hany and R. Nüesch, *Environ. Sci. Technol.*, 1996, 31, 240-247.

24. S. B. Haderlein, K. W. Weissmahr and R. P. Schwarzenbach, *Environ. Sci. Technol.*, 1996, 30, 612-622.

25. P. D. Christian, A. R. Richards and T. Williams, *Appl. Environ. Microbiol.*, 2006, 72, 4648-4652.

26. D. H. Taylor, R. S. Moore and L. S. Sturman, *Appl. Environ. Microbiol.*, 1981, 42, 976-984.

27. S. M. Lipson and G. Stotzky, *FEMS Microbiol. Lett.*, 1986, 37, 83-88.

28. C. V. Kumar and G. L. McLendon, *Chem. Mat.*, 1997, 9, 863-870.

29. C. V. Kumar and A. Chaudhari, *J. Am. Chem. Soc.*, 2000, 122, 830-837.

30. C. V. Kumar and A. Chaudhari, *Microporous Mesoporous Mat.*, 2003, 57, 181-190.

31. R. D. Misra, C. Nune, T. C. Pesacreta, M. C. Somani and L. P. Karjalainen, *Acta Biomater.*, 2013, 9, 6245-6258.

32. C. Nune, R. D. Misra, M. C. Somani and L. P. Karjalainen, *J. Biomed. Mater. Res. Part A*, 2014, 102, 1663-1676.

33. K. C. Nune and R. D. K. Misra, *J. Biomed. Nanotechnol.*, 2014, 10, 1320-1335.

34. R. D. K. Misra and C. Nune, *Mater. Technol.*, 2014, 29, B41-B48.

35. A. Naidja and P. M. Huang, *Journal of Molecular Catalysis A: Chemical*, 1996, 106, 255-265.

36. I. Lozzi, L. Calamai, P. Fusi, M. Bosetto and G. Stotzky, *Soil Biology and Biochemistry*, 2001, 33, 1021-1028.

37. S. Roe, *Protein Purification Applications: A Practical Approach*, Oxford University Press, 2001.

38. A. K. Pavlou and M. J. Belsey, *Eur. J. Pharm. Biopharm.*, 2005, 59, 389-396.

39. A. K. Pavlou and J. M. Reichert, *Nat. Biotechnol.*, 2004, 22, 1513-1519.

40. J.-J. Lin, J.-C. Wei, T.-Y. Juang and W.-C. Tsai, *Langmuir*, 2006, 23, 1995-1999.

41. C. Mousty, *Appl. Clay Sci.*, 2004, 27, 159-177.

42. T.-Y. Tsai, S.-S. Huang, and C.-C. Hsu, Patent No. US 8,741,619 B1, Jun. 3, 2014.

43. V. W.-K. Wu, *Chem. Lett.*, 2006, 35, 1380-1381.

44. V. W.-K. Wu and F. Kure, *Chin. J. Chem.*, 2010, 28, 2520-2526.

45. V. W.-K. Chao (Wu), *Chin. J. Chem. Phys.*, 2013, 26, 295-302.

46. C.-C. Hsu, V. W.-K. Chao (Wu), S.-H. Huang, C. Chan, T.-C. Wu, P.-H. Wang, T.-Y. Tsai, *J. Chinese Chem. Soc.* (Submission, Dec.2014).

Figure captions

Figure 1. Dispersions of inorganic layered materials CL5, CL42, CL120, CL88, CL111, CL22, and MgAl- LDH in an aqueous solution.

Figure 2. Adsorptions of inorganic layered materials dependent on the BSA molecular concentrations at 1 – 6 corresponding to 15 – 90 mg of BSA, respectively, and mixed with 15 mg of every kind of 6 purchased clays and synthesized MgAl-LDH. Measurements of adsorptions by 6 clays and MgAl-LDH were done at pH = 2.5 and 9.5, respectively.

Figure 3. Adsorption of BSA molecules in mg by using inorganic layered smectite material CL42 in g at pH = 2.50, 4.70, and 9.50. CL42 was chosen, because it showed the optimalst saturation adsorption and increase of the interlayer spacing for BSA (Table 1).

Figure 4. X-ray diffraction patterns (WAXD) of the BSA-intercalated clays CL42, CL120, CL111, CL22, and CL88. Every sample BSA/clay was a mixture with clay 15 mg and BSA 15 mg, in weight proportion 1:1 and at pH = 2.5.

Figure 5. X-ray diffraction patterns (WAXD) of the BSA-intercalated clay CL111, which was chosen as one of the octahedrally substituted smectites (Table 1), at different

concentrations of 15 – 75 mg BSA and mixed with clay 15 mg, distinguishable with 1/1, 2/1, 3/1, 4/1, and 5/1, respectively.

Figure 6. X-ray diffraction patterns (WAXD) of the BSA-intercalated clay CL5 as tetrahedrally substituted smectite (Table 1), at different concentrations of 15 – 75 mg BSA and mixed with clay 15 mg, distinguishable with 1/1, 2/1, 3/1, 4/1, and 5/1, respectively, and pure CL5, at pH = 2.5.

Figure 7. Dark grey strips as the peeling off structures from the TEM images of BSA/CL5 (5/1), where the weight proportion between BSA and CL5 was 5:1, represented as 5/1.

(a) x50 K and 100 nm, (b) x100 K and 50 nm.

Figure 8. TGA of pure CL5 (0/1) and BSA/CL5 (5/1). Samples of pure CL5 and BSA/CL5 were prepared in the phosphate buffer solution at pH = 2.5. Pure CL5 keeps stable up to temperature 900 ^{O}C, and much more stable than the mixture of CL5 and BSA. Weight reduction 5.96 % at 200 ^{O}C and 67.86 % at 900 ^{O}C should come from the vaporization of water and the adsorbed BSA molecules on the surfaces of interlayers of BSA/CL5, respectively.

Figure 9. FT-IR relative transmission spectra of (a) pure CL5 and (b) CL5 and BSA after adsorption of BSA with concentration in weight of BSA 75 mg and CL5 15 mg (5/1).

Figure 10. X-ray diffraction patterns (WAXD) of mixtures MgAl-LDH and BSA after adsorption of BSA with different concentrations 1/1, 2/1, 3/1, 4/1, and 5/1, corresponding weight, 15, 30, 45, 60, and 75 mg.

Scheme 1. Synthesis procedure of MgAl-LDH.

Scheme 2. Procedure for adsorption and intercalation of BSA.

Scheme 3. Adsorption Patterns of BSA (in yellow) in Inorganic Layered Materials (in sheet form). There are three groups 1. Octahydrally substituted smectited CL111, CL42, CL22, CL120, and CL88; 2. Tetrahedrally substituted smectited CL5; and 3. MgAl-LDH investigated. ionic exchange capacities (IEC) of low, suitable and high are shown from left to right. BSA/Clay concentrations 0/1, 1/1, 2/1, 3/1, 4/1, and 5/1 with the respective d-spacings are shown from left to right.

Table 1. Properties of Inorganic Layered Materials and the BSA-intercalated inorganic layered materials.

Table 2. Information of clay materials

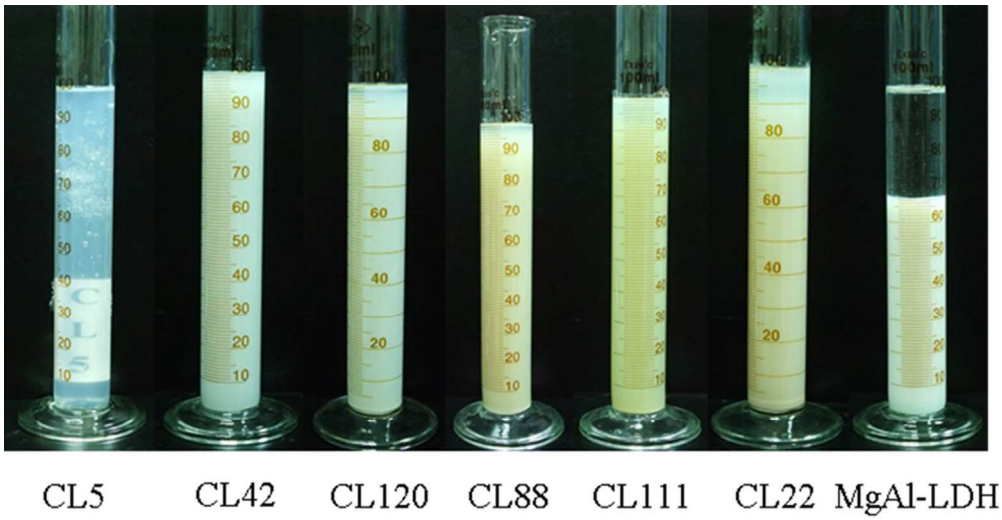

Figure 1. Dispersions of inorganic layered materials CL5, CL42, CL120, CL88, CL111, CL22, and MgAl- LDH in an aqueous solution.
82x42mm (300 x 300 DPI)

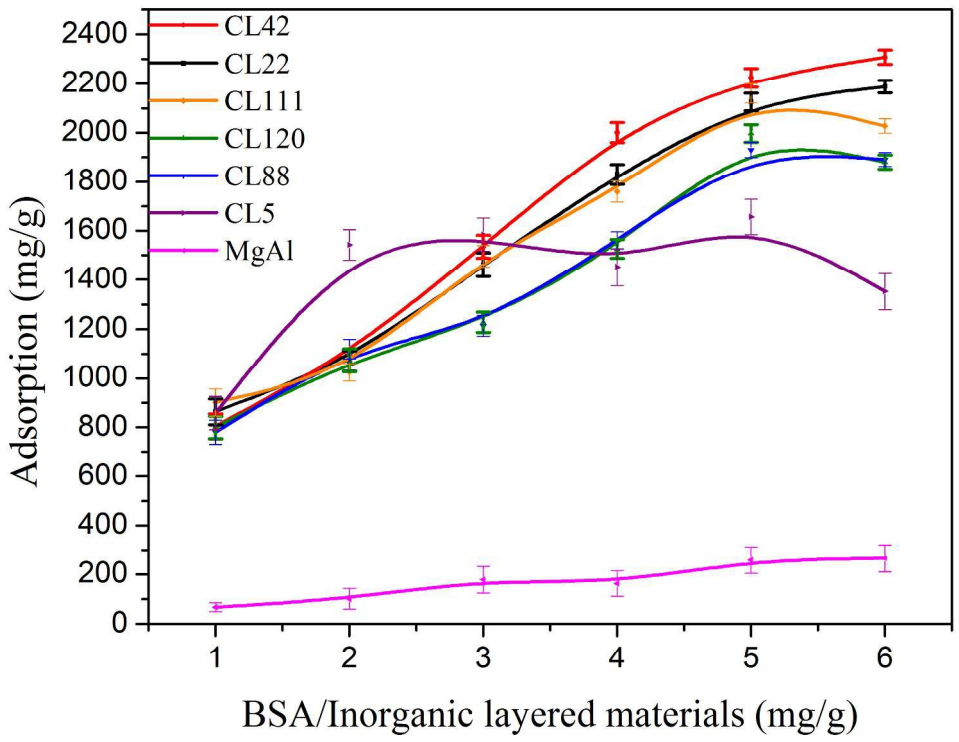

Figure 2. Adsorptions of inorganic layered materials dependent on the BSA molecular concentrations at 1 – 6 corresponding to 15 – 90 mg of BSA, respectively, and mixed with 15 mg of every kind of 6 purchased clays and synthesized MgAl-LDH. Measurements of adsorptions by 6 clays and MgAl-LDH were done at pH = 2.5 and 9.5, respectively.
238x181mm (300 x 300 DPI)

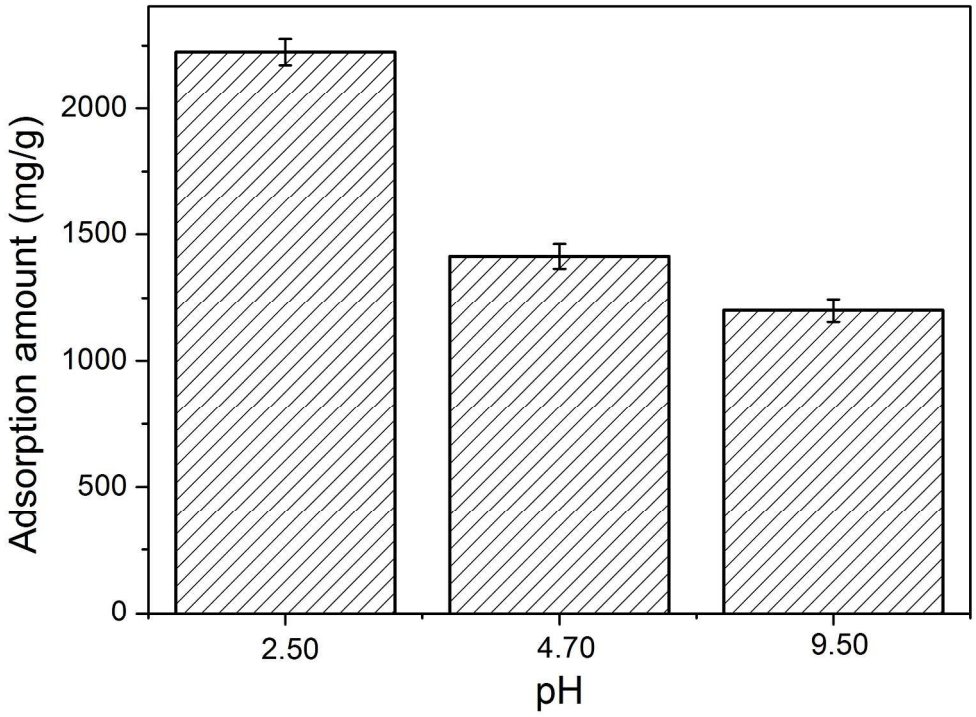

Figure 3. Adsorption of BSA molecules in mg by using inorganic layered smectite material CL42 in g at pH = 2.50, 4.70, and 9.50. CL42 was chosen, because it showed the optimalst saturation adsorption and increase of the interlayer spacing for BSA (Table 2).
240x175mm (300 x 300 DPI)

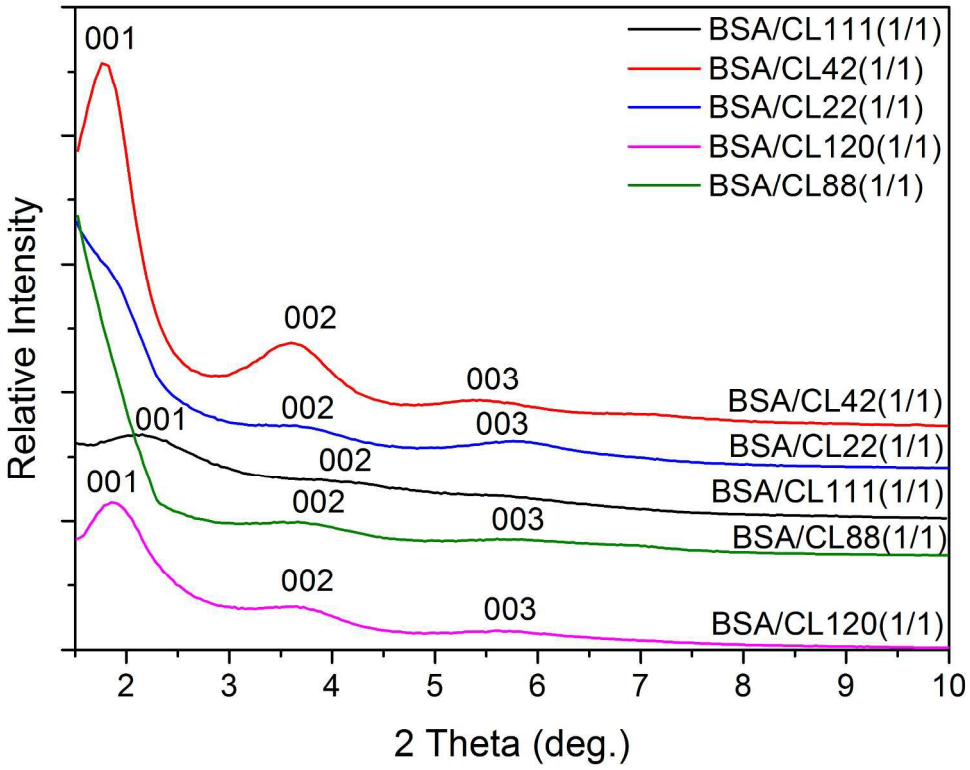

Figure 4. X-ray diffraction patterns (WAXD) of the BSA-intercalated clays CL42, CL120, CL111, CL22, and CL88. Every sample BSA/clay was a mixture with clay 15 mg and BSA 15 mg, in weight proportion 1:1 and at pH = 2.5.
225x176mm (300 x 300 DPI)

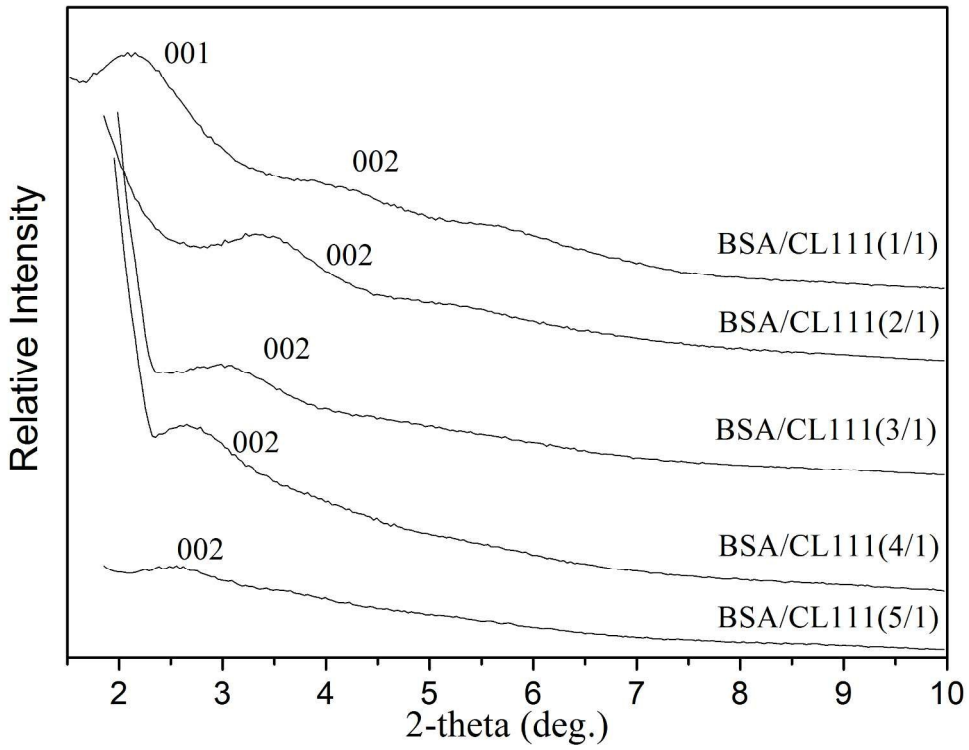

Figure 5. X-ray diffraction patterns (WAXD) of the BSA-intercalated clay CL111, which was chosen as one of the octahedrally substituted smectites (Table 2), at different concentrations of 15 – 75 mg BSA and mixed with clay 15 mg, distinguishable with 1/1, 2/1, 3/1, 4/1, and 5/1, respectively.
222x174mm (300 x 300 DPI)

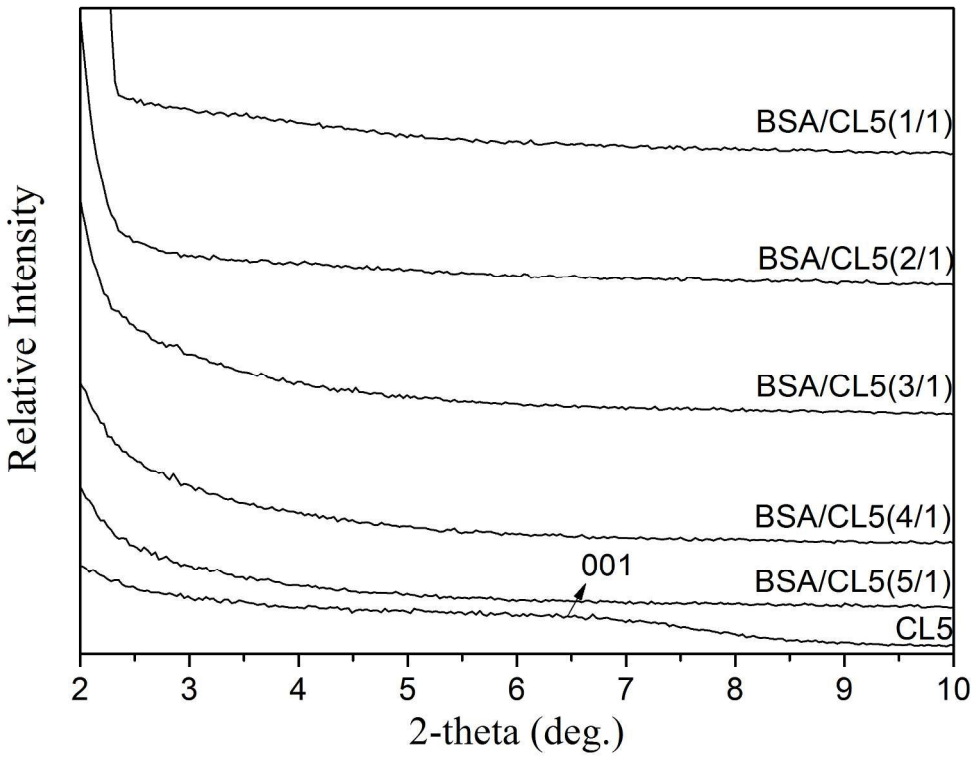

Figure 6. X-ray diffraction patterns (WAXD) of the BSA-intercalated clay CL5 as tetrahedrally substituted smectite (Table 2), at different concentrations of 15 – 75 mg BSA and mixed with clay 15 mg, distinguishable with 1/1, 2/1, 3/1, 4/1, and 5/1, respectively, and pure CL5, at pH = 2.5.
226x176mm (300 x 300 DPI)

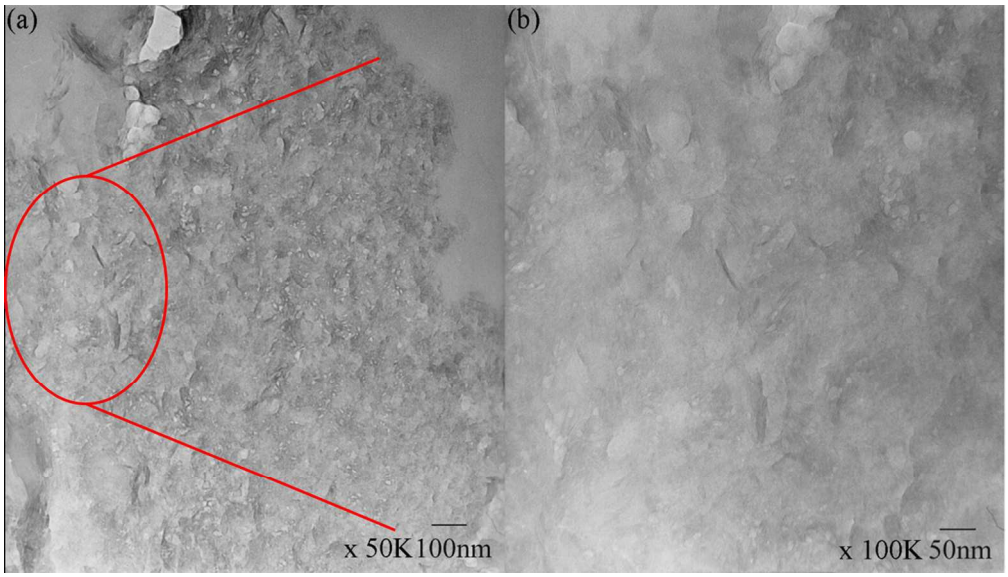

Figure 7. Dark grey strips as the peeling off structures from the TEM images of BSA/CL5 (5/1), where the weight proportion between BSA and CL5 was 5:1, represented as 5/1.
(a) x50 K and 100 nm, (b) x100 K and 50 nm.
96x54mm (600 x 600 DPI)

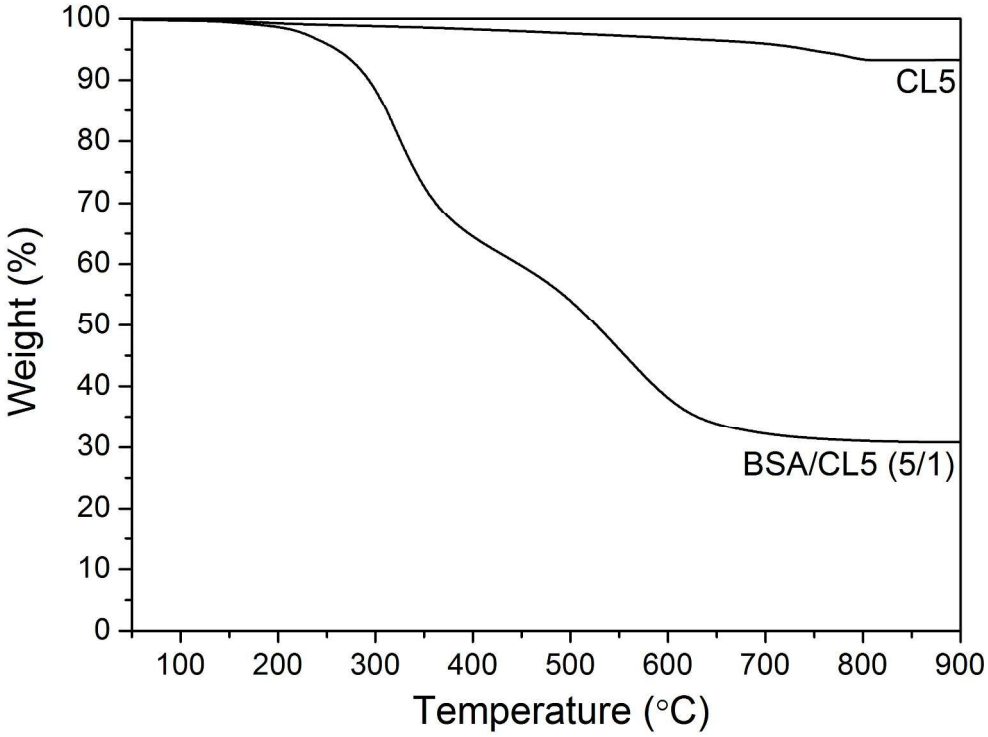

Figure 8. TGA of pure CL5 (0/1) and BSA/CL5 (5/1). Samples of pure CL5 and BSA/CL5 were prepared in the phosphate buffer solution at pH = 2.5. Pure CL5 keeps stable up to temperature 900 ºC, and much more stable than the mixture of CL5 and BSA. Weight reduction 5.96 % at 200 ºC and 67.86 % at 900 ºC should come from the vaporization of water and the adsorbed BSA molecules on the surfaces of interlayers of BSA/CL5, respectively.
238x178mm (300 x 300 DPI)

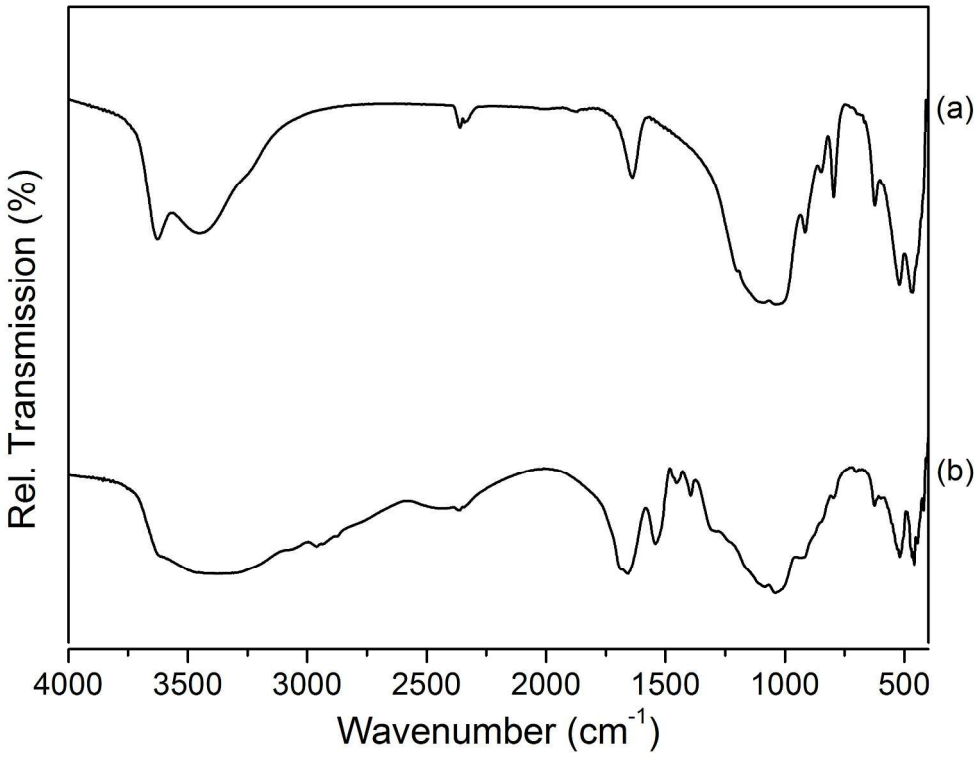

Figure 9. FT-IR relative transmission spectra of (a) pure CL5 and (b) CL5 and BSA after adsorption of BSA with concentration in weight of BSA 75 mg and CL5 15 mg (5/1).
229x175mm (300 x 300 DPI)

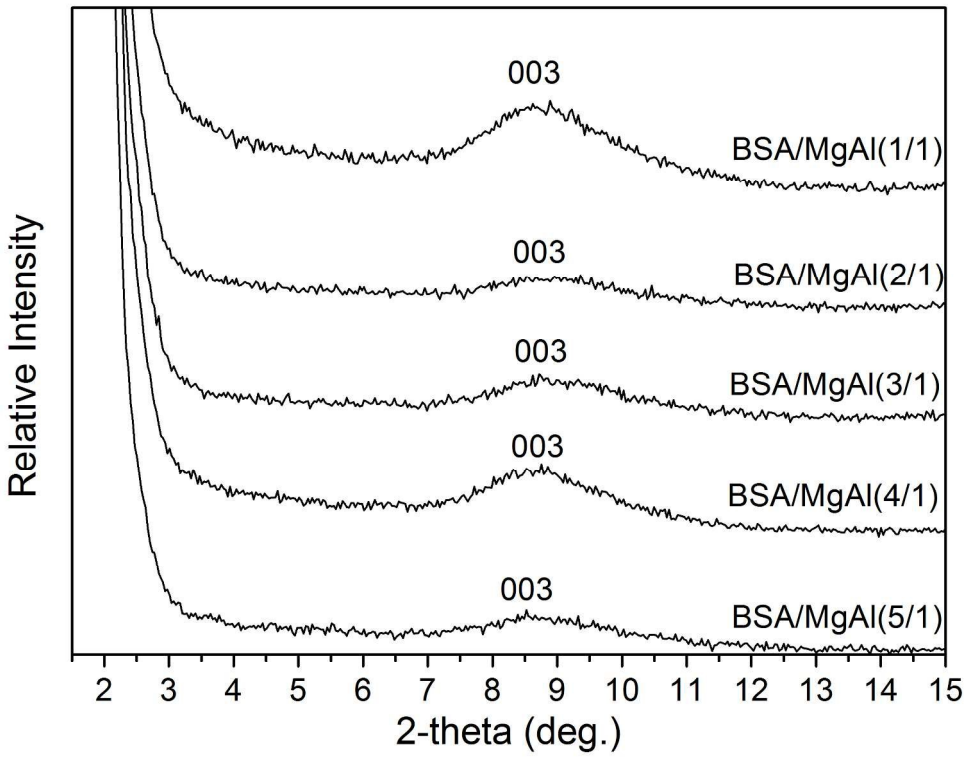

Figure 10. X-ray diffraction patterns (WAXD) of mixtures MgAl-LDH and BSA after adsorption of BSA with different concentrations 1/1, 2/1, 3/1, 4/1, and 5/1, corresponding weight, 15, 30, 45, 60, and 75 mg.
225x173mm (300 x 300 DPI)

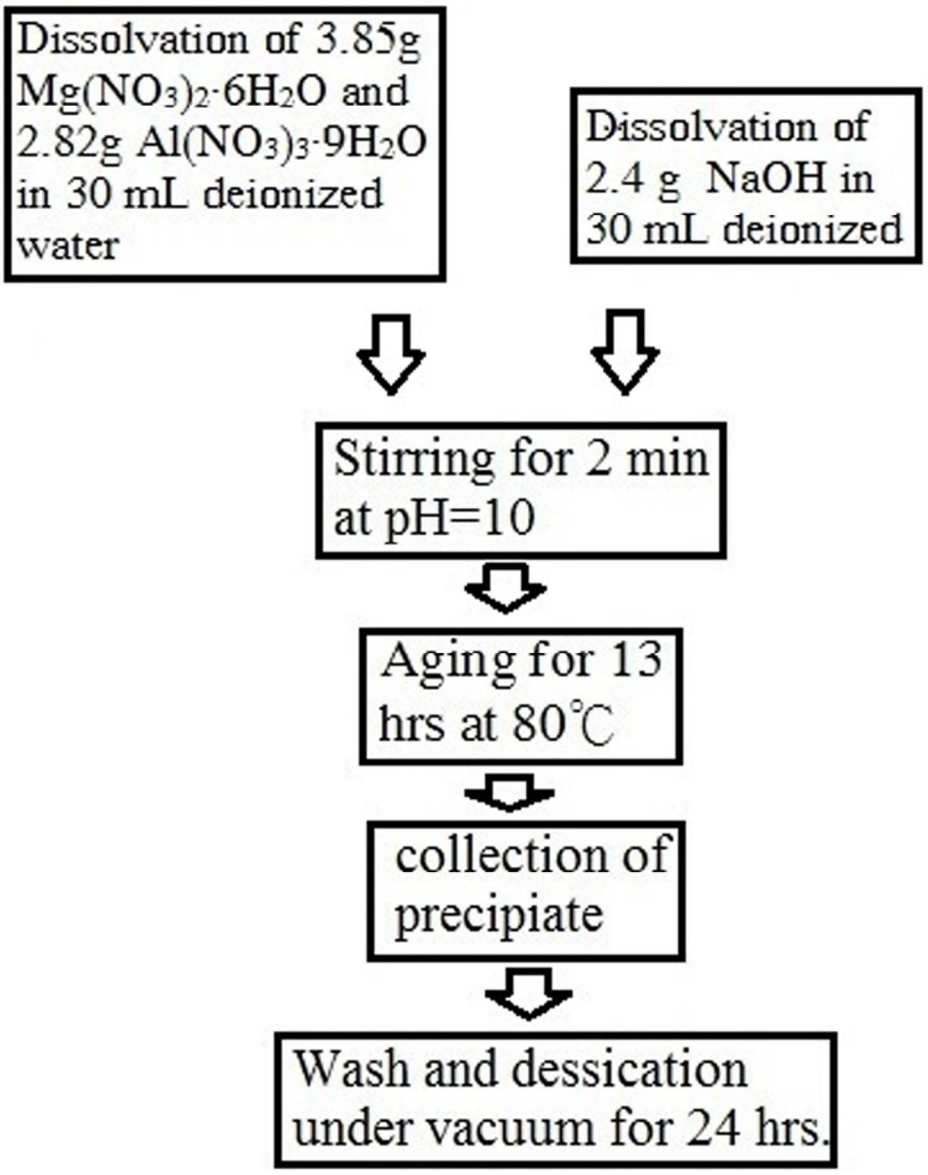

Scheme 1. Synthesis procedure of MgAl-LDH.
85x107mm (300 x 300 DPI)

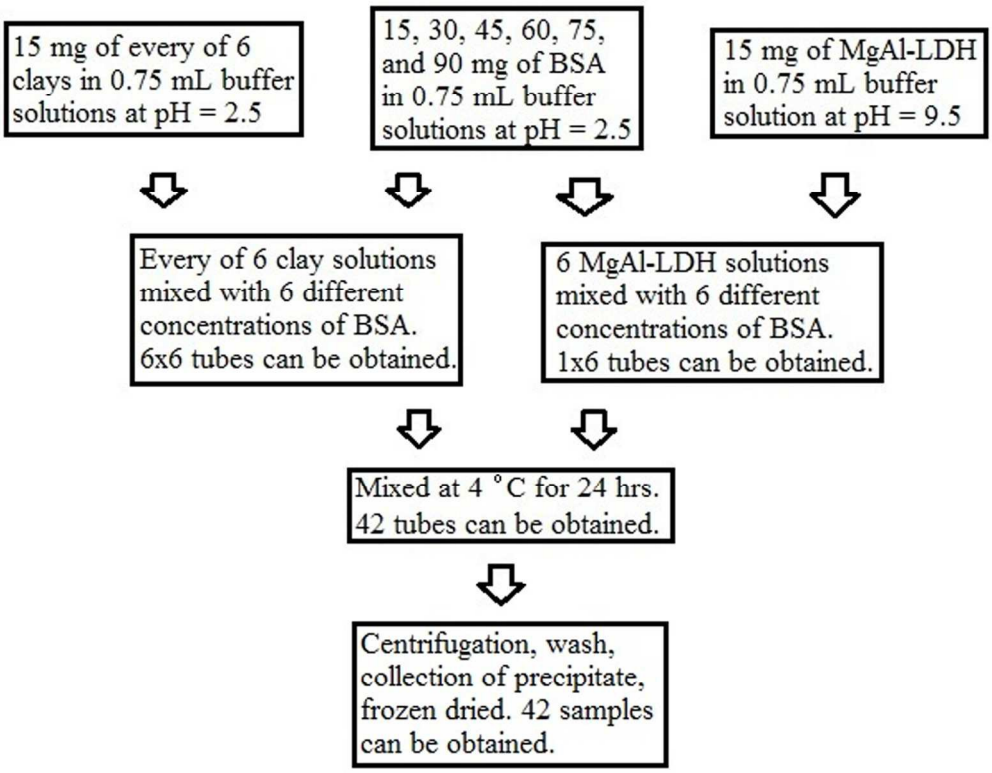

Scheme 2. Procedure for adsorption and intercalation of BSA.
139x108mm (300 x 300 DPI)

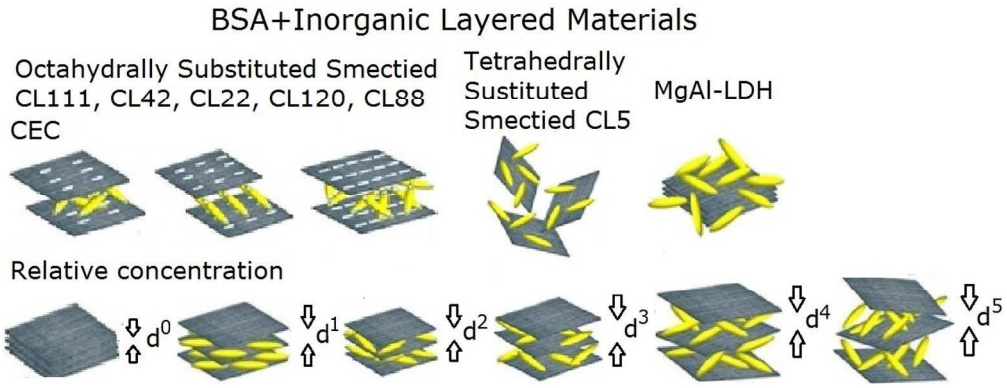

Scheme 3. Adsorption Patterns of BSA (in yellow) in Inorganic Layered Materials (in sheet form). There are three groups 1. Octahydrally substituted smectited CL111, CL42, CL22, CL120, and CL88; 2. Tetrahedrally substituted smectited CL5; and 3. MgAl-LDH investigated. ionic exchange capacities (IEC) of low, suitable and high are shown from left to right. BSA/Clay concentrations 0/1, 1/1, 2/1, 3/1, 4/1, and 5/1 with the respective d-spacings are shown from left to right.
294x112mm (300 x 300 DPI)

Table 1. Properties of inorganic layered materials and the BSA-intercalated inorganic layered materials

inorganic layered materials	CL111	CL42	CL22	CL120	CL88	CL5	MgAl
Charges distribution	Octahedral substituted smectites					Tetrahedral substituted smectites	LDH
IEC[a]	92	116	140	168	200	75	380
Swellability[b]	92	100	90	98	95	100	67
Saturation Adsorption[c]	2161±39	2224 ±37	2125 ±36	1997 ±36	1930 ±31	1656±72	258 ±53
BSA/inorganic layered material[d]	pH Averaged d-spacing as well as interlayer spacing (Å)						
0/1	12.38	13.12	12.93	12.61	12.45	13.81	26.58
1/1	43.16	50.14	47.36	47.41	48.83	--*	30.12
2/1	52.68	63.26	56.56	55.34	59.82	--*	30.12
3/1	59.22	71.74	64.82	67.6	64.54	--*	30.45
4/1	66.58	73.52	71.16	72.00	78.95	--*	31.05
5/1	72.02	80.46	79.13	77.15	79.20	--*	31.65
6/1	-	-	-	-	-	-	-

[a] meq/100 g of inorganic layered material.

[b] mL/2g of inorganic layered material.

[c] Adsorbed BSA in mg by 1 g of inorganic layered material.

[d] BSA/inorganic layered material are 0, 15, 30, 45, 60, and 75 mg BSA mixed with 15 mg of every kind of inorganic layered materials distinguishable with 0/1, 1/1, 2/1, 3/1, 4/1, and 5/1, respectively, prepared for WAXD, where 6/1 was not done.

[*] no signal detection

Table 2. Information of clay materials

inorganic layered materials	Chemical Formula	Provider	Purity
CL111	$(Na, Ca)_{0.66}(Al, Mg)_4Si_8O_{20}(OH)_4 \cdot nH_2O$	Southern Clay Products Co. Ltd.	99 %
CL22	$Na_{1.10}(Al_{2.90}Fe_{0.30}Mg_{0.8})Si_8O_{20}(OH)_4 \cdot H_2O$	Nanocor Co. Ltd.	99 %
CL42	$Na_{0.89}(Al_{3.11}Mg_{0.89})\ Si_8O_{20}(OH)_4 \cdot 1.75H_2O$	PAI KONG Nanotechnology Co. Ltd.	99 %
CL120	$Ca_{0.31}Na_{0.07}$ $(Al_{3.31}Mg_{0.69})Si_8O_{20}(OH)_4 \cdot 2.148H_2O$	China Glaze Co. Ltd.	99 %
CL88	$Ca_{0.54}Na_{0.12}(Al_{2.8}Mg_{0.77}\ Fe_{0.43})Si_8O_{20}$ $(OH)_4 \cdot 0.34H_2O$	China Glaze Co. Ltd.	99 %
CL5	$Na_{0.49}Mg_{0.14}(Mg_{5.97}Al_{0.03})(Si_{7.20}Al_{0.80})O_{20}(OH)_4 \cdot nH_2O$	Kunimine Co. Ltd.	99 %

Graphical Abstract

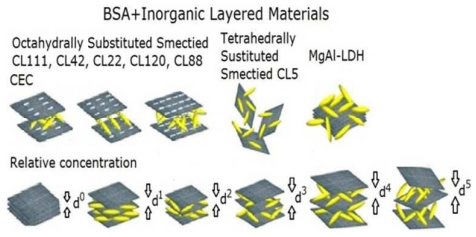	Adsorption patterns of BSA (in yellow) in Inorganic Layered Materials (in sheet form) of Group 1. Octahydrally substituted smectited CL111, CL42, CL22, CL120, and CL88; 2. Tetrahedrally substituted smectited CL5; and 3. MgAl-LDH have been investigated (Scheme 1 and Fig. 2). Cation exchange capacities (CEC) of low, suitable and high; BSA/Clay concentrations 0/1, 1/1, 2/1, 3/1, 4/1, and 5/1 with the respective d-spacings from left to right (Table 2) are shown.